Available online at www.sciencedirect.com
ScienceDirect
Journal of Power Sources 163 (2007) 933–942
JOURNAL OF POWER SOURCES
www.elsevier.com/locate/jpowsour

A flow channel design procedure for PEM fuel cells with effective water removal

Xianguo Li *, Imran Sabir, Jaewan Park

Department of Mechanical Engineering, University of Waterloo, Waterloo, Ontario N2L 3G1, Canada

Received 29 August 2006; received in revised form 3 October 2006; accepted 4 October 2006
Available online 13 November 2006

Abstract

Proper water management in polymer electrolyte membrane (PEM) fuel cells is critical to achieve the potential of PEM fuel cells. Membrane electrolyte requires full hydration in order to function as proton conductor, often achieved by fully humidifying the anode and cathode reactant gas streams. On the other hand, water is also produced in the cell due to electrochemical reaction. The combined effect is that liquid water forms in the cell structure and water flooding deteriorates the cell performance significantly. In the present study, a design procedure has been developed for flow channels on bipolar plates that can effectively remove water from the PEM fuel cells. The main design philosophy is based on the determination of an appropriate pressure drop along the flow channel so that all the liquid water in the cell is evaporated and removed from, or carried out of, the cell by the gas stream in the flow channel. At the same time, the gas stream in the flow channel is maintained fully saturated in order to prevent membrane electrolyte dehydration. Sample flow channels have been designed, manufactured and tested for five different cell sizes of 50, 100, 200, 300 and 441 cm^2. Similar cell performance has been measured for these five significantly different cell sizes, indicating that scaling of the PEM fuel cells is possible if liquid water flooding or membrane dehydration can be avoided during the cell operation. It is observed that no liquid water flows out of the cell at the anode and cathode channel exits for the present designed cells during the performance tests, and virtually no liquid water content in the cell structure has been measured by the neutron imaging technique. These measurements indicate that the present design procedure can provide flow channels that can effectively remove water in the PEM fuel cell structure.

Keywords: PEM fuel cells; Flow channel design; Water flooding; Neutron imaging technique

1. Introduction

Global and local environmental degradation and health danger associated with the emissions of fossil fuel combustion call for alternative fuels and energy sources for sustainable development, and decreasing fossil fuel reserves has also placed energy security among the national agenda. Polymer electrolyte membrane (PEM) fuel cells have been regarded as environmentally friendly power source for transportation, stationary co-generation and portable applications, and are compatible with alternative fuels and renewable energy sources for sustainable development and energy security [1,2]. Life cycle analysis indicates the advantage of PEM fuel cells in both higher overall energy efficiency and lower emissions [3,4]. However, dynamic water balance and management have imposed one of the dormant technical challenges for PEM fuel cell design and operation, and have direct consequence on the performance and lifetime of PEM fuel cell systems.

The importance of the water balance and management arises from the fact that the polymer membrane electrolyte used in PEM fuel cells requires full hydration in order to maintain good performance and lifetime, and the guarantee of the membrane hydration under the full operating conditions has been achieved, with a good degree of success, by supplying fully humidified reactant gas streams for both anode and cathode [1]. However, water is produced in the cathode as a result of electrochemical reaction, and water is also transported from the anode to the cathode through the membrane electrolyte via the electroosmotic drag effect. Water transport also occurs due to the local gradients of the pressure and concentration. Consequently, liquid water flooding occurs if water is not removed adequately from the cell (cathode in particular). Water flooding will make the PEM fuel cell performance unpredictable, unreliable and

* Corresponding author. Tel.: +1 519 888 4567x36843.
E-mail address: x6li@uwaterloo.ca (X. Li).

0378-7753/$ – see front matter © 2006 Elsevier B.V. All rights reserved.
doi:10.1016/j.jpowsour.2006.10.015

unrepeatable under the nominally identical operating conditions, and elaborate experimental diagnostics and schemes need to be implemented to achieve consistent results with much lower performance and limiting current densities [5,6]. Therefore, water management has become a delicate task, both too much or too little water can adversely impact the performance and lifetime of PEM fuel cells. Maintaining a perfect water balance during dynamic operation process has posed a significant challenge for PEM fuel cell design and operation, and hence water management becomes a critical issue for PEM fuel cells.

A number of active and passive methods have been investigated to tackle this critical issue of water management, and the most successful of them is through the appropriate design of flow channels built on the flow field (bipolar) plates [1,7,8]. Among the flow channel layouts investigated [8], serpentine flow channel layout [9,10] is the most widely known and used, often regarded as "industry standard", since under the same operating and design conditions PEM fuel cells with serpentine flow channels tend to have the best performance and durability/reliability. Recent numerical and experimental investigation [11–13] indicates that for serpentine flow channels, the reactant gas experiences a pressure drop and concentration change along the channel; since the channel cross-section is small, in the order of 1 mm × 1 mm or smaller, while the channel length is very long, in the order of meters, the pressure drop at the corresponding location between the adjacent channels becomes substantial, significant pressure gradient is thus set up across the porous electrode, much larger than the pressure gradient along the channel direction, resulting in considerable cross leakage flow between the adjacent channels. This significant cross leakage flow through the porous electrode induces a strong convection in the electrode, bringing the reactant gas to the catalyst layer for electrochemical reaction and remove the product water from the reaction sites and electrodes, in a way similar to the flow set up in an interdigitated flow channel [14–17], responsible for the better overall cell performance when using the serpentine flow channels.

However, serpentine flow channel layout is not the ideal flow field configuration, and has a number of problems. First, it typically results in a relatively long reactant flow path, hence a substantial pressure drop, consequently significant parasitic power loss associated with the cathode air supply (as much as over 35% of the stack output power). Second, significant decrease of reactant concentration occurs from the flow channel inlet to the outlet, leading to considerable Nernst losses for practical cells of large sizes. Most important of all, the use of serpentine flow channel layout often causes the membrane dehydration near the channel inlet region, while liquid water flooding occurs for a significant region near the channel exit due to excessive liquid water carried downstream by the reactant gas stream and collected along the flow channel [18]. These issues have caused the often-observed phenomenon of achieving good performance for small cells, and poor performance for apparently the same cells with large sizes, and are primarily responsible for the difficulty in establishing scaling laws for PEM fuel cells. As noticed by Wang et al. [19], reactant gases with inlet relative humidity less than 100% for single serpentine flow channel layout would result in a loss of performance at low current density, an indication of membrane dehydration. Flow fields for dry reactants or less than 100% relative humidity operations have been suggested, in fact, desired, but at the cost of low cell performance and high platinum loading [20]. It should also be emphasized that along with flow channel layout, channel dimensions and specifications of other cell components also influence the water removal and performance of the cell [21].

Typically, the cooling flow channels are kept substantially the same, if not completely the same, as the flow channels for the anode and cathode reactant gas streams. Thus, serpentine flow channels for the reactant gas streams and coolant flows tend to create a low temperature region near the channel inlet, and a high temperature region near the channel outlet. This temperature gradient along the flow channel not only affects the cell performance, complicating water management, but also creating difficulty for thermal management and cell sealing [22]. This is because all fuel cells have best performance when the entire cell is at the same uniform temperature [1], and high temperature also shortens the lifetime for the sealing materials around the cell periphery [22]. Therefore, an ideal flow channel design should provide a uniform concentration of reactants and a uniform temperature over the electrode surface, a reasonably small pressure drop from the channel inlet to the channel outlet to minimize the parasitic losses, a mechanism to maintain membrane hydration over the entire cell, avoiding membrane hydration near the channel inlet; and a mechanism for the effective removal of liquid water in the porous electrode structure to prevent water flooding of the cell near the flow channel outlet.

In the present study, a methodology has been developed for the design of flow channels for PEM fuel cells, including channel layout, configuration, channel cross-section and channel length. The channel design incorporates the PEM fuel cell structures and operating conditions. Sample flow channels have been designed, manufactured and tested for both performance and water removal capability. Experimental measurements of cell performance are made for five different cell active sizes of 50, 100, 200, 300 and 441 cm^2. Neutron imaging technique is used for in situ measurements of water content in the cell structure. Experimental results demonstrate that for the present flow channel design water flooding phenomenon is effectively prevented, and cell performance is reliable and repeatable for the same nominal operating conditions.

2. Design of flow channels

There are many varieties of flow field layouts for bipolar plates that have been developed and patented [8], but there is little information in the open literature regarding the design procedure or methodology for the channel length and cross-sectional dimensions as well as the pressure drops for flows in the channels. In this section, a general procedure for the flow channel design will be described by using the fundamental concepts of flow through rectangular ducts or pipes for a given active area of PEM fuel cells as an illustrative example. The operating conditions of the PEM fuel cells are taken into account for the design process.

2.1. Channel layout: general

First and foremost important in the channel design is the layout or configuration of the flow channels. From the literature review and experimental observations, the serpentine flow channel layout, which can be considered as many parallel flow channels connected in series, can provide excellent cell performance due to its balanced capability of water removal and acceptable pressure drop (parasitic loss) [9,10,13]. Therefore, serpentine flow channels are considered in this study in illustrating the design procedures involved.

2.2. Channel cross-section: shape and dimensions

A flow channel can have almost endless choices of the cross-sectional shape, from the simple rectangular or square shape, to triangular, trapezoidal, semi-circular shape or any other shape that might be desired [1]. For the conventional bipolar plate, graphite is typically the material used, which is hard and brittle, and hence difficult to machine the flow channels on it. As a result, the making of the flow channels on the bipolar plate is time-consuming and expensive process, making up the majority of the cost for a completed bipolar plate, which contributes significantly to the total cost of a PEM fuel cell stack [8]. From the cost consideration and the ease of channel fabrication, the geometrical shape of the channel cross-section has traditionally be chosen as either rectangular or square, and we will consider these two shapes in illustrating the design procedure for the flow channels in this study, as shown in Fig. 1.

The channel width a is often chosen based on the need for distributing the reactant gas over the active cell surface, and is ideally the larger the better from the mass transfer consideration. The distance between the channel, or the width of the land, w, is decided based on the need for current collection (the transport of electrons), and is ideally the larger the better from the electron transfer consideration. Both the transport processes for the electrons and reactant gas to and/or from the catalyst layer are influenced by the structure and the properties of the electrode, or the so-called gas-diffusion layer (GDL) [23,24]. The channel depth b is determined based on the consideration of the flow regime and the flow condition in the channel, the channel length and the pressure drop in the channel, etc. Therefore, the design or selection of the flow channel dimensions should consider the cell operating conditions as well as the cell structural parameters. Typically, the GDL and bipolar plate materials are highly conductive electronically, while the reactant gas transport is relatively slower, hence the ratio of the land width to the channel width is typically in the range of 0.8–1.0.

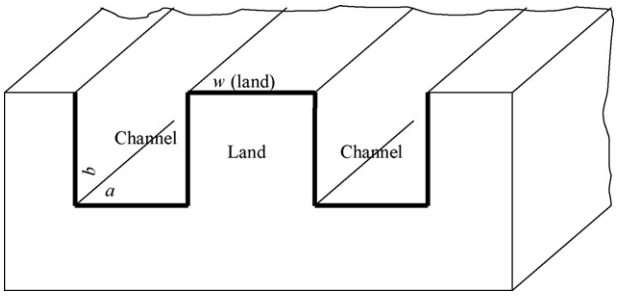

Fig. 1. Channel cross-section view.

2.3. Flow regime in the channel

Because bipolar plates are required to be good electrical collectors, and to provide mechanical support for the fragile membrane-electrode assemblies (MEA), small flow channels are typically utilized along with small intervals between the neighboring channels, such as the rectangular flow channel shown in Fig. 1. This couples with the typical cell operating conditions, yielding the anode and cathode gas flows in the laminar flow regime. It is also possible that the cathode gas flow might even reach the transition regime from the laminar to turbulent flow. Due to the flow intermittency, transition flow regime is almost always avoided in practical applications. Although turbulent flow has an enhanced ability to transport mass and heat, it also results in a higher pressure drop [25], leading to a high parasitic loss. On the other hand, a typical laminar flow is more than sufficient to provide the mass transport of the reactant gases into the electrode for fuel cell electrochemical reactions under the most extreme fuel cell operating conditions (high current densities) [1]. Further, fluctuations inherent in turbulent flows may also impact PEM fuel cell performance since PEM fuel cells can respond almost instantaneously to the changes in the concentration [26]. Therefore, it is conventional to design the flow channels in such a manner that both the anode and cathode gas flows are maintained laminar in the channel, i.e., low Reynolds number flows [1,27].

2.4. Channel length

For internal flows such as the ones in fuel cell flow channels, Reynolds number is conventionally defined as [25]

$$Re_{D_h} = \frac{\text{Inertial force}}{\text{Viscosity}} = \frac{\rho V D_h}{\mu} \tag{1}$$

where ρ is the density, μ the viscosity of the gas in the flow channel and V is the mass averaged velocity in the channel, determined by

$$V = \frac{\dot{m}}{\rho A_c} \tag{2}$$

where $\dot{m}$ is the mass flow rate in the channel and D_h is the hydraulic diameter of the channel. For a non-circular cross-section flow channel, such as the rectangular channel shown in Fig. 1, D_h is defined as [25]

$$D_h = \frac{4A_c}{P} \tag{3}$$

where the cross-sectional area is equal to the product of the side length

$$A_c = ab \tag{4}$$

and the wetted perimeter is

$$P = 2(a + b) \tag{5}$$

To guarantee the flow remains in the laminar flow regime, the maximum Reynolds number should be kept in the order of 2000 [25]. On the other hand, to maintain sufficient flow convection, the minimum Reynolds number should be in the order of 100 or above. For laminar flow, the accepted correlation for the hydrodynamic entrance length is [25]

$$\frac{L_e}{d} \approx 0.06Re \tag{6}$$

As mentioned earlier, the flow channel is typically small in its cross-sectional dimension, about 1 mm × 1 mm or smaller; and is typically very long, about meters or longer. Therefore, for the typical Reynolds number range indicated above, the entrance region can be neglected in the first calculation for the flow channel design.

In fluids engineering, the pressure drop for a flow in a channel of length L is conventionally expressed through the following equation:

$$\Delta p = f\frac{L}{D_h}\frac{\rho V^2}{2} \tag{7}$$

where the friction factor f for steady fully developed laminar flows in a channel with square cross-section is given as [25]

$$f = \frac{56.91}{Re_{D_h}} \tag{8}$$

Substituting the above relation into Eq. (7), and considering Eqs. (1)–(5), the pressure drop can be written, for flow channels with square cross-section ($a = b$), as

$$\Delta p = 28.455\left(\frac{\mu\dot{m}}{\rho}\right)\left(\frac{L}{a^4}\right) \tag{9}$$

Then the flow channel length can be determined, for flow channels with square cross-section, as

$$L = \frac{\Delta p\rho a^4}{28.455\mu\dot{m}} \tag{10}$$

Similarly, the flow channel length for channels with rectangular cross-section can be derived as

$$L = \frac{8\Delta p\rho(ab)^3}{C\mu\dot{m}(a+b)^2} \tag{11}$$

where $C = fRe_{D_h}$ is a function of the aspect ratio b/a for rectangular flow channels, and is available in literature, e.g. [25].

Therefore, the flow channel length can be determined from the above Eqs. (10) and (11) if the channel cross-sectional dimensions, the reactant mass flow rate related to the set fuel cell operating conditions as well as the pressure drop, required for the specific conditions of fuel cell operation, are known. The channel cross-sectional dimensions are considered in Section 2.2, and the reactant mass flow rate and the appropriate pressure drop are considered in the next section.

2.5. Determination of pressure drop

The pressure drop for the gas mixture in the flow channel of a PEM fuel cell is defined as

$$\Delta p = p_{T,in} - p_{T,exit} \tag{12}$$

where p_T is the total pressure of the reactant gas stream, equal to the sum of the partial pressures for the reactant gas (hydrogen or reformed gas for the anode and air for the cathode) and water vapor, assuming the gas mixture behaves like an ideal gas. The subscripts "in" and "exit" represent the pressure value at the inlet and exit of the flow channel, respectively.

The total pressure of the reactant gas stream at the channel inlet or exit is typically set according to the operating conditions for the PEM fuel cells, but not both. For the present design consideration, with no loss of generality, we consider the case that the total pressure of the reactant gas stream at the channel inlet, or simply inlet pressure, is set according to the operating conditions for the PEM fuel cell. As pointed out early, a significant performance limitation for the PEM fuel cells is the liquid water flooding of the cathode electrode, especially at high current density (hence high power density) operation, and an important aim for the cathode flow channel design is to remove sufficient amount of water to avoid the water flooding phenomena. Although water flooding of the anode does occur in reality for improperly designed flow channels, its impact on the cell performance is much less than the corresponding impact of flooding the cathode. Hence, the cathode flow channel design is described in detail here, and the anode flow channel can be designed similarly by following the same procedure. Assuming ideal gas behavior, the total pressure at the cathode channel exit, which is needed to remove all the water in the cathode in vapor form, can be determined from the following relation:

$$\frac{p_{w,exit}}{p_{T,exit} - p_{w,exit}} = \frac{\dot{N}_{w,exit}}{\dot{N}_{air,exit}} \tag{13}$$

where $p_{w,exit}$ is the partial pressure of the water vapor at the cathode channel exit. To avoid removing excessive amount of water that would cause the dehydration of the membrane electrolyte, $p_{w,exit}$ should be set equal to the saturation pressure of water vapor at the channel exit, which is determined by the local temperature at the channel exit.

To determine the total pressure at the channel exit from Eq. (13), the molar flow rate of the water vapor and air at the cathode channel exit, $\dot{N}_{w,exit}$ and $\dot{N}_{air,exit}$, needs to be determined first. From the preceding considerations, for a properly designed cathode flow channel the gas mixture at the channel exit would be fully saturated without the presence of liquid water. Hence,

$$\dot{N}_{w,exit} = \dot{N}_{w,in} + \dot{N}_{w,prod} \tag{14}$$

where the water molar flow rate at the channel inlet, $\dot{N}_{w,in}$, is determined by the relative humidity of the inlet gas stream as well as the total inlet pressure and the cell operating temperature. Again assuming ideal gas behavior for the gas mixture at the cathode channel inlet, and similar to Eq. (13), the molar flow

rate of the water at the channel inlet becomes

$$\dot{N}_{w,in} = \dot{N}_{air,in}\left(\frac{p_{w,in}}{p_{T,in} - p_{w,in}}\right) \quad (15)$$

where $P_{w,in}$ is the partial pressure of water vapor at the channel inlet, evaluated according to the relative humidity set for the inlet gas mixture and the saturation pressure of water vapor corresponding to the cell operating temperature.

On the other hand, $\dot{N}_{w,prod}$ is the molar flow rate corresponding to the net amount of water production in the cathode, equal to the combined effect of water production due to the oxygen reduction reaction at the cathode, the electroosmotic drag that transports water from the anode to the cathode, the back diffusion due to the gradient of water concentration across the membrane electrolyte, the pressure differential between the anode and cathode stream, and any condensation/evaporation of water due to the local temperature variation. Hence, the determination of the exact amount of the net water production requires much detailed analysis, or it can be determined experimentally such as through the overall water balance or by neutron imaging technique [26,27]. With no loss of generality in illustrating the procedures involved, we can consider in a first attempt (with understanding that the actual design calculation may require iterative approach) only the effect of water production in the cathode due to oxygen reduction reaction, or

$$\dot{N}_{w,prod} = \frac{JA}{n_w F} \quad (16)$$

where J is the current density of the PEM fuel cell, A the active area of the cell, n_w the number of moles of electron transferred per mole of water formed in the cathode oxygen reduction reaction, or $n_w = 2$ and $F = 96{,}487\,\mathrm{C\,mol^{-1}}$ equivalent is the Faraday constant.

The molar flow rate of the air at the cathode channel exit is simply the difference between the amount of inflow at the channel inlet and the amount of oxygen consumed in the cell due to the oxygen reduction reaction, or

$$\dot{N}_{air,exit} = \dot{N}_{air,in} - \dot{N}_{O_2,consumed} \quad (17)$$

The air flow rate at the channel inlet can be evaluated based on the stoichiometry of the oxygen and the current drawn from the cell as follows:

$$\dot{N}_{air,in} = \frac{JA}{n_{O_2} F} n_{air}\,St_{O_2} \quad (18)$$

where n_{O_2} is the number of moles of electron transferred per mole of oxygen consumed in the PEM fuel cell, and $n_{O_2} = 4$; n_{air} is the number of moles of air per mole of oxygen in the air, and $n_{air} = 4.773$ [1]. For PEM fuel cells, the amount of oxygen (hence air) supplied to the cells is conventionally expressed in terms of a parameter called the oxygen stoichiometry, defined as

$$St_{O_2} = \frac{\dot{N}_{O_2,in}}{\dot{N}_{O_2,consumed}} = \frac{\text{Molar flow rate of oxygen supplied to the cell}}{\text{Molar flow rate of oxygen consumed in the cell}} \quad (19)$$

Therefore, the amount of oxygen consumed in the cell can be determined as follows:

$$\dot{N}_{O_2,consumed} = \frac{JA}{n_{O_2} F} \quad (20)$$

The mass flow rate of the reactant gas in the cathode channel inlet and exit are obtained from the molar flow rate given in Eqs. (17) and (18), multiplied by the mean molecular weight of the gas mixture. The latter is calculated by the molecular weight of the species (oxygen, nitrogen and water vapor) weighted by their respective mole fraction that changes from the channel inlet to the channel exit.

Now the formulation is complete for the determination of the flow channel length that can remove the right amount of water to avoid liquid water flooding of the cathode electrode as well as the dehydration of the membrane electrolyte. For a given cell operation, the cell operating temperature, pressure, cell current density and the oxygen stoichiometry are specified, and then the pressure drop required can be calculated. From the pressure drop the flow channel length required is determined accordingly. The present formulation can easily be implemented on a computer for the iterative design calculation. For the present study, an Excel worksheet was developed for the iterative calculations for various selections of the channel cross-section, the active cell area and the flow channel layout/configuration.

2.6. Geometry of the channel layout

Consider a PEM fuel cell with a rectangular active area specified by the side length H_1 and H_2 as shown in Fig. 2. A single serpentine flow channel traverses the active cell surface with a

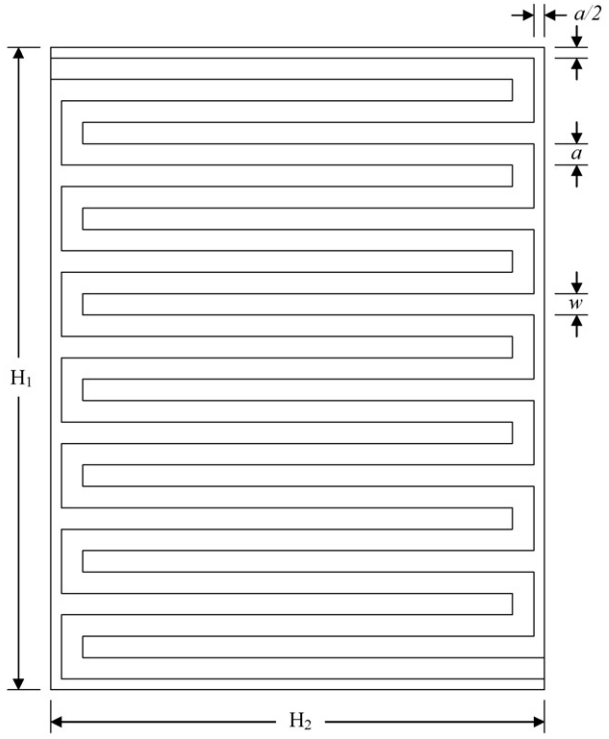

Fig. 2. Illustration of the serpentine flow channels.

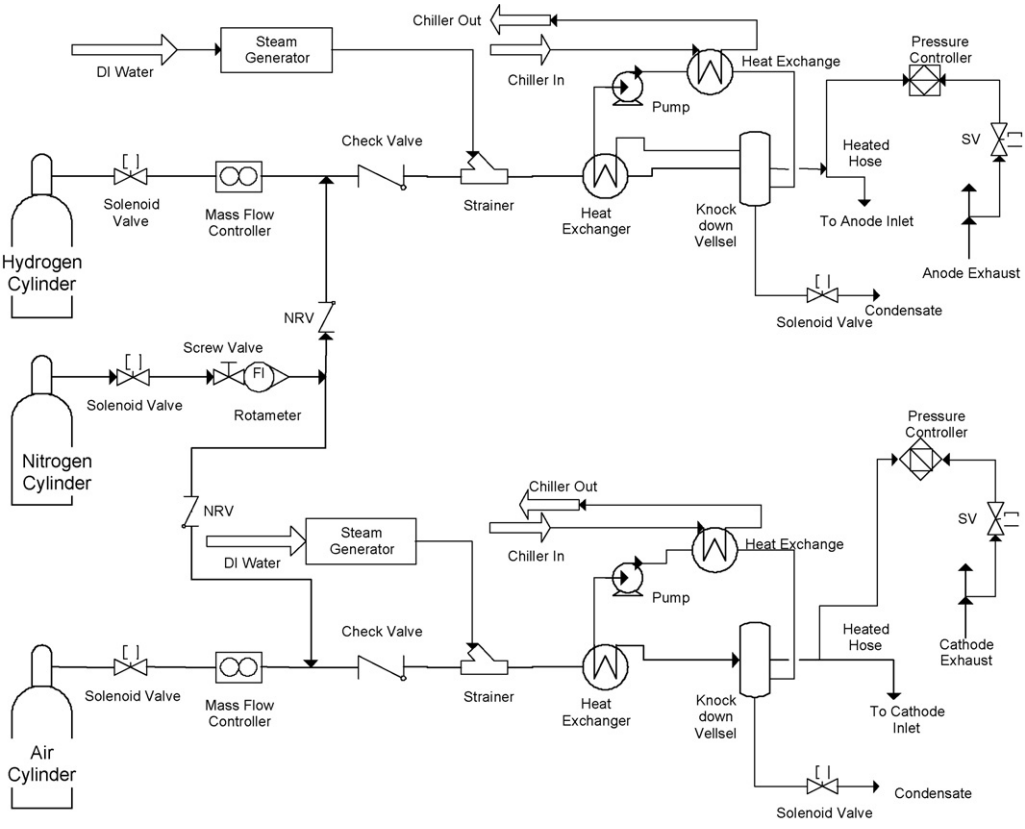

Fig. 3. Schematic of FCATS operation.

recess of $a/2$ (or a margin of $a/2$ all around). Recall a is the channel width, and the land width is denoted as w. As pointed out early, such a serpentine flow channel could be considered as many parallel channels connected in series, then the number of channels connected in parallel is identical to the number of the turns for the serpentine channel. The total channel length is composed of the length of the each parallel channels connected in series, the length in the channel turn or connection regions as well as the extra channel length associated with the inlet and exit region, and can be determined geometrically as follows:

$$L = (H_2 - 2a)n_{ch} + (w + a)(n_{ch} - 1) + 2a \tag{21}$$

where n_{ch} is the number of the serpentine channel turns, and it can be obtained geometrically again by considering the side length H_1 of the active cell area:

$$H_1 = an_{ch} + w(n_{ch} - 1) + a$$

or

$$n_{ch} = \frac{H_1 - a + w}{a + w} \tag{22}$$

On the other hand, the total channel length determined from Eqs. (11) and (21) must be identical, and this requirement will provide the channel depth b.

3. Procedure for design calculations

The design calculation starts with the specification of the cell active sizes (H_1 and H_2), and the cell operating conditions (temperature, pressure, stoichiometry for both hydrogen

Table 1
Calculated dimensions and associated flow parameters for the sample flow channel designs

Active cell size (cm^2)	50	100	200	300	441
Active cell dimensions, H_1 (mm) × H_2 (mm)	71 × 71	100 × 100	136 × 136	175 × 175	210 × 210
Channel dimensions, a (mm) × b (mm) × w (mm)	0.8 × 0.8 × 0.8	1 × 1.1 × 1	0.85 × 0.9 × 0.8	0.9 × 0.8 × 0.9	0.8 × 1 × 0.75
No. of serpetine channels	1	1	3	5	7
Reynolds number, Re	1310	1980	1460	1450	1500
Ratio of channel depth to width, b/a	1	1.1	1.05	0.89	1.25
Estimated hydrodynamic entrance length, L_e (mm)	62.8	41.5	76.8	76.3	77.5
Ratio of entrance length to total channel length, L_e/L (%)	1.91	1.66	2	1.98	1.91
Calculated channel length, L (m)	3.28	4.78	3.83	3.85	4.05
Actual length measured on the plate (m)	3.195	5.1	3.618	3.287	3.952

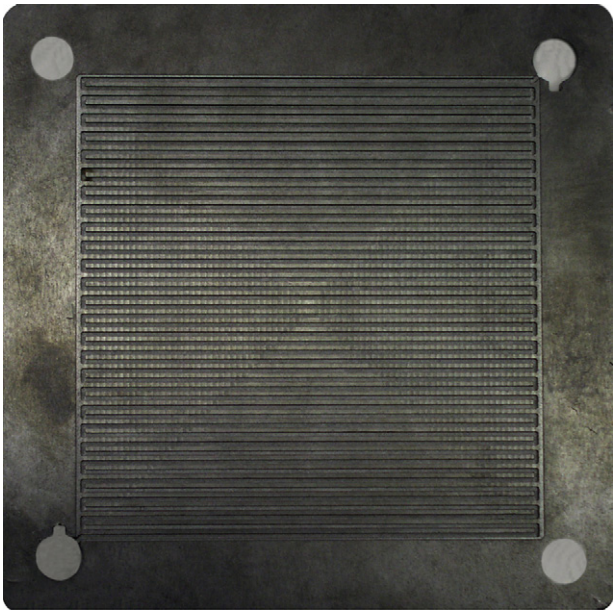

Fig. 4. Picture of the designed flow channels machined on the bipolar plate.

and oxygen, as well as the cell current density). Then the proper pressure drop needed is calculated as described in Section 2.5. The next step is the selection of the channel width a, and the land width w (based on the ratio w/a chosen based on the consideration of the relative importance of the mass and electron transport as well as the mechanical integrity of the cell, etc.). The channel depth b is calculated by equating the total channel length expressed in Eqs. (11) and (21). Finally, the channel length L is calculated from either Eqs. (11) and (21). It must be emphasized that check must be made to ensure that the flow Reynolds number indeed remains in the laminar flow regime.

Although this procedure of the design calculation seems to be straightforward, in reality, iterative calculation is required due to a number of reasons. First the pressure drop in the flow channel is contributed by not only the frictional loss, but also the so-called minor losses associated with the change in the flow direction [27], that occurs in the channel turn regions. Second, the frictional loss coefficient f is influenced by the mass suction or injection at the electrode surface due to the reactant gas going into the electrode for electrochemical reaction and the water vapor coming out of the electrode surface [30,31]. Third, the net amount of water produced in the electrode is influenced by the dynamic water transport and electrochemical reaction, and significant effort is often required to determine [30,31]. All these effects depend on many design and operating conditions, such as the properties of the electrode used (thickness, porosity and/or hydraulic permeability), the operating temperature, pressure, stoichiometry, current density, etc. However, the general theory formulated in the previous section is of significance to PEM fuel cell community, and the specific modifications considering the above effects will have to be determined for the specific PEM fuel cell or stack design and operation.

4. Experimental setup

In spite of the difficulty, a design calculation procedure has been implemented in an Excel worksheet, and flow channels have been designed for the active cell areas of 50, 100, 200, 300 and 441 cm^2. These designs have been fabricated and experimental measurements have been made of the PEM fuel cell performance. Graphite was used for these flow field plates. All MEAs were manufactured using Nafion® 115 membrane loaded with 0.53 mg Pt cm^{-2}. The catalyst deposition was made by proprietary ink formulation of catalyst deposited on a proprietary tape casting support material. The gas diffusion media (GDL) was SGL Carbon Sigracet 10BB. The thickness of GDL was 16.5 mil (16.5/1000 in.) with porosity of 84%. The specific electrical resistance of this GDL material in the through-plane direction is 10 mΩ cm^2. The material is hydrophobicized substrate with a 5 wt% PTFE loading and has a micro porous layer on one side. Aluminum alloy 6061 was chosen for end plates and current collectors were made of copper alloy.

The FCATS fuel cell test system from Hydrogenics Inc. used in this experimental work consists of a gas sub-system, electronic load box and a computer running a controlling and data logging software (HyWare®). For the automatic control and running of the tests, text scripts can also be written in Hydrogenics Automation Language (HyAL™). The test station has the capability of setting and maintaining required operating conditions of the fuel cell within close limits. Parameters like pressure, temperature, flow rate, relative humidity, etc., can be controlled by user-friendly Lab-View-based interface touch screen. Numbers of important read backs are also displayed on various screens along with the front of the test station. The test station is also controlled by a number of safety features, which make it reasonably safe under test conditions of pressurized air and hydrogen streams.

De-ionized (DI) water is used for reactant humidification, and chiller water is supplied for temperature control and relative humidity setting of the reactant gas streams. Pressurized gas streams (pressure > 680 kPa) are fed to the test station supply inlets for the proper functioning of the control system and valves operation. A required flow rate of the gas is set through the user interface software touch screen and fully automated system supply the exact amount of flow within ±1% of the full scale flow into the common header. The DI water on the other hand is filtered and supplied to a 1.5 kW bubbler steam generator from where steam is injected into the supply stream of gas. According to the set amount of relative humidity (RH) extra amount of water vapor is condensed into moisture separator, through which chiller water is circulated. The condensate is purged out of the test station. This humidified stream of gas or reactant is then heated to the required temperature in the heated hose and is ready to supply to the fuel cell. The cell temperature is maintained with a separate flexible heater controlled through the FCATS. The pneumatic pressure controller on the supply line maintains the backpressure after the outlet of the fuel cell. Fig. 3 illustrates the main operational functions of FCATS.

Another experiment has been carried out by using neutron imaging technique [28] to measure the liquid water content inside the PEM fuel cell structure in order to validate the effectiveness of the present designs in water removal. The details of the experiment are given elsewhere [29].

5. Results and discussion

As stated early, flow channels have been designed for the active cell areas of 50, 100, 200, 300 and 441 cm^2, and the active areas are all in square form. In the present study, the flow channels are designed according to the following conditions:

- cell current density $J = 0.65\ A\ cm^{-2}$,
- stoichiometry of air = 2.0,
- stoichiometry of hydrogen = 1.2,
- inlet pressure (P_{in}) = 3 atma,
- operating temperature = 80 °C,

and the designed flow channel dimensions and associated flow parameters are presented in Table 1. Notice that the calculated channel length represents the length calculated as outlined above for the design procedure, and the actual length measured on the plate represents the length measured after the channel was machined on the bipolar plate; these two lengths should be identical in theory, but they differ slightly representing the fact that the flow channel layout designed by using AutoCAD deviates slightly from the design intention. Since the difference between the two is sufficiently small it is considered acceptable. For the small active cell sizes of 50 and 100 cm^2, a single serpentine flow channel traverses throughout the active area. However, for

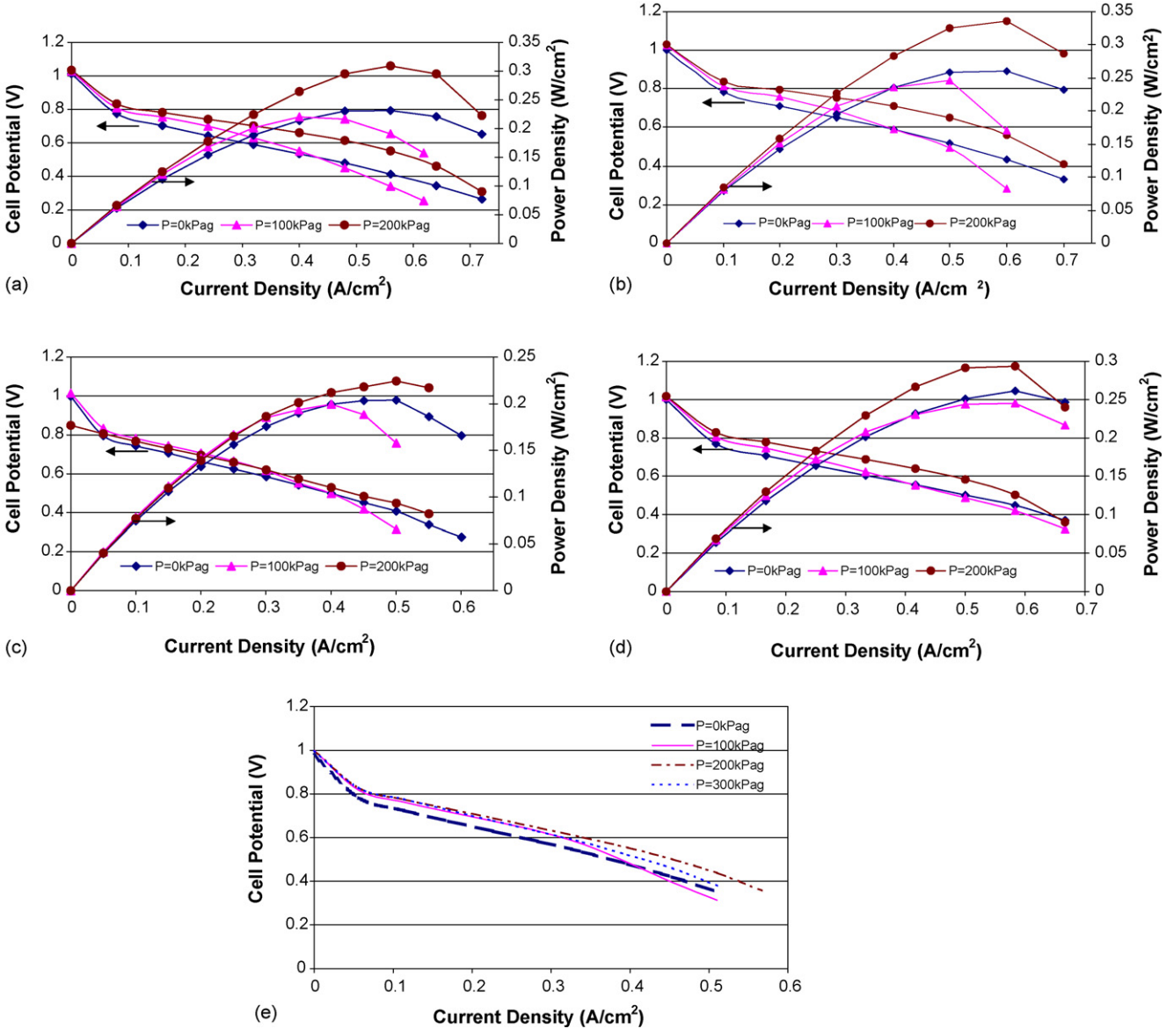

Fig. 5. Experimentally measured PEM fuel cell performance for different cell active sizes: (a) 50 cm^2; (b) 100 cm^2; (c) 200 cm^2; (d) 300 cm^2 and (e) 441 cm^2. Experimental conditions: cell operating temperature of 80 °C, air stoichiometry of 3, hydrogen stoichiometry of 1.5, relative humidity of 100% for both anode and cathode gas streams at the channel inlets.

the other three cell sizes a single serpentine flow channel will result in turbulent flow in the channel, as a result, multiple parallel serpentine channels are used. Another consideration in the design is to make the channel inlet and exit locate on the opposite corners in order to achieve cross-flow arrangement so that the problem of air and hydrogen inlet ports overlaying on top of each other is avoided. Fig. 4 illustrates the designed flow channels machined on the bipolar plate for the present experimental measurements.

Fig. 5 shows the experimentally measured performance of PEM fuel cells with the designed flow channels. Notice that the hydrogen and air stroichimetries of 1.5 and 3 are larger than the designed values listed earlier. However, this is done so on purpose because the actual pressure drop through the flow channels is lowered due to the cross leakage flow between the adjacent flow channels [12,13], and can be compensated for by the higher flow rates for the anode and cathode gas streams. On the other hand, a parametrical measurement indicates that the impact on the cell performance is minimal when the hydrogen stoichiometry is increased from 1.2 to 1.5 and air stoichiometry is increased from 2 to 3 [11]. Despite the common knowledge that PEM fuel cell performance would decrease significantly when the active cell sizes are increased, it might be observed that the present cell performance remains fairly similar for the five different active cell areas from 50 to 441 cm^2. Due to the limitation of the present test equipment on the flow rates and load box, the measured data for the largest cell size of 441 cm^2 shown in Fig. 5(e) are also limited in the current density measured. From Fig. 5(a–e), it is seen that the best performance is achieved at the operating pressure of 200 kPa (gauge), equivalent to the designed operating pressure of 3 atm (absolute). Although one might argue that higher pressure would yield better performance based on theoretical analysis, Fig. 5(e) suggests that performance actually become worsen as the operating pressure is further increased to 300 kPa (gauge) from 200 kPa (gauge). These all indications that the present designs were able to achieve the intended "water flooding" free operation, or at least reduced impact of "water flooding" phenomenon. Although during the test it was not possible to observe directly if the cells were indeed free of "water flooding", it was possible to observe at the cell exit through the transparent tubing that there was no liquid water flowing out of the cell. On the other hand, for a flooded cell it is easy to observe liquid water flowing out of the cell exit, especially when the cell is shaken [5].

To further investigate the existence of liquid water in the cell structure, neutron imaging technique has been used to measure the amount of liquid water in the tested cell [29], as shown in Fig. 6. A single serpentine flow channel is used for both anode and cathode side. The anode (horizontal) and cathode (vertical) flow channels are arranged in cross flow, so that the anode inlet and exit are located at the lower right and top left corners, respectively; and the cathode inlet and exit are located at the top right and lower left corners, respectively. It is seen that the present cell is indeed virtually free of liquid water in the cell structure (virtually black color), as shown in Fig. 6(a). As a comparison, Fig. 6(b) illustrates the presence of liquid water (white and blue colors) in the cell for improperly designed flow channels so that

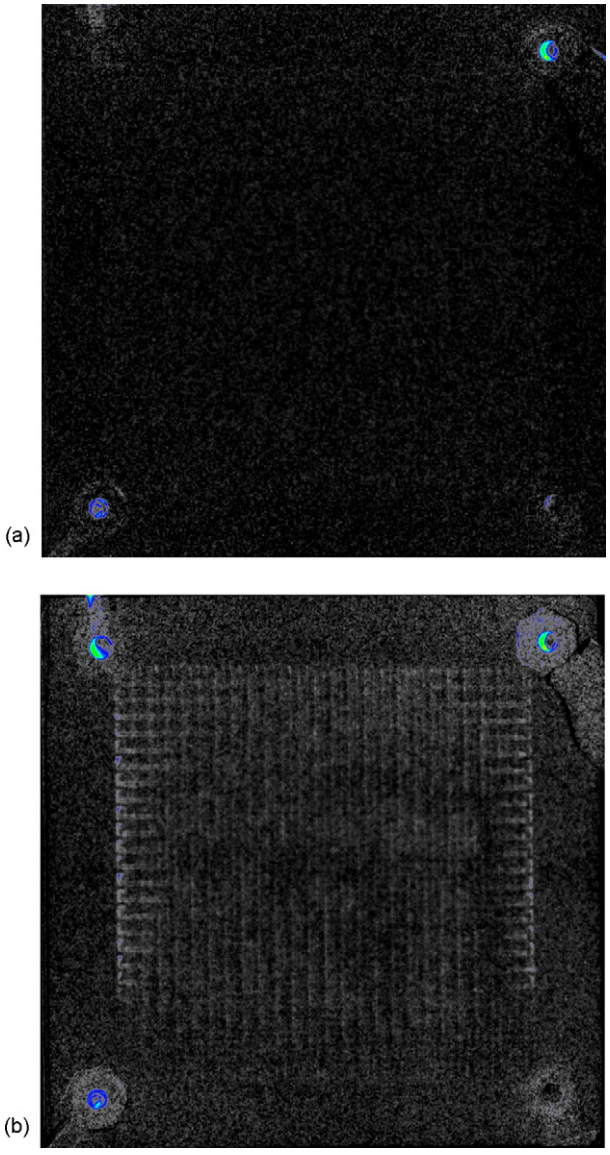

Fig. 6. Pictures of PEM fuel cells taken by the neutron imaging technique. (a) Virtually no water is shown for the present designed flow channels and (b) liquid water is present almost over the entire cell's active area for improperly designed flow channels. For both case a single serpentine flow channel is adopted for both anode and cathode side. The anode and cathode flow channels are arranged in cross flow with the anode inlet and exit located at the lower right and top left corners, and the cathode inlet and exit located at the top right and lower left corners.

water was not removed adequately (water has accumulated in the cell). Fig. 6(b) also reveals that liquid water is present in both the anode and cathode flow channels, suggesting that liquid water flooding can occur for both anode and cathode if the flow channels are not properly designed.

6. Conclusions

In the present study, a design procedure has been developed for flow channels in PEM fuel cells. The main design philosophy is based on the determination of an appropriate pressure drop along the flow channel so that all the liquid water in the cell

is evaporated and removed from or carried out of the cell by the gas stream in the flow channel. On the other hand, the gas stream in the flow channel is maintained fully saturated in order to prevent membrane electrolyte dehydration. Sample flow channels have been designed, manufactured and tested for five different cell sizes of 50, 100, 200, 300 and 441 cm^2. Similar cell performance has been measured for these five significantly different cell sizes, indicating that scaling of the PEM fuel cells is possible if liquid water flooding or membrane dehydration can be avoided during the cell operation. The effectiveness of the present flow channel designs in water removal is confirmed by two different experimental observations. The first is that no liquid water flows out of the cell at the anode and cathode channel exits for the present designed cells; and the second is the measurement of liquid water content in the cell structure by the neutron imaging technique. Therefore, it might be concluded that the present design procedure has been reasonably validated and its effectiveness in water removal capability reasonably confirmed.

Acknowledgements

This study was supported by Ontario Research and Development Challenge Fund (ORDCF) via CAMM (Centre for Automotive Materials and Manufacturing), DuPont Canada, Auto21 Network of Centres of Excellence program, DaimlerChrysler, NIST and the Natural Sciences and Engineering Research Council of Canada (NSERC).

References

[1] X. Li, Principles of Fuel Cells, Taylor & Francis, New York, 2006.
[2] X. Li, Energy Policy 33 (2005) 2237–2243.
[3] N. Zamel, X. Li, J. Power Sources 155 (2006) 297–310.
[4] N. Zamel, X. Li, J. Power Sources, 2006, doi:10.1016/j.jpowsour.2006.08.007.
[5] A. Mughal, X. Li, Int. J. Environ. Stud. 63 (2006) 377–389.
[6] X.G. Yang, N.A. Burke, C.Y. Wang, K. Tajiri, K. Shinohara, J. Electrochem. Soc. 152 (2005) A759–A766.
[7] C. Cavalca, S.T. Homeyer, E. Walsworth, US Patent No. 5,686,199 (1997).
[8] X. Li, I. Sabir, Int. J. Hydrogen Energy 142 (2004) 134–153.
[9] D.S. Watkins, K.W. Dircks, D.G. Epp, US Patent No. 4,988,583 (1991).
[10] D.S. Watkins, K.W. Dircks, D.G. Epp, US Patent No. 5,108,849 (1992).
[11] I. Sabir, Experimental investigation of proton exchange membrane fuel cells. M.A.Sc. Thesis, University of Waterloo, Waterloo, Ontario, Canada, 2005.
[12] T. Kanezaki, X. Li, J.J. Baschuk, J. Power Sources 162 (2006) 415–425.
[13] J. Park, X. Li, J. Power Sources 163 (2007) 853–863.
[14] D.L. Wood, J.S. Yi, T.V. Nguyen, Electrochim. Acta 43 (1998) 3795–3809.
[15] A. Kazim, H.T. Liu, P. Forges, J. Appl. Electrochem. 29 (1999) 1409–1416.
[16] V. Gurau, F. Barbir, J.K. Neutzler, US Patent No. 6,551,736 (2003).
[17] F. Issacci, T.J. Rehg, US Patent No. 6,686,084 (2004).
[18] C.Y. Wang, Chem. Rev. 104 (2004) 4727–4766.
[19] L. Wang, A. Husar, T. Zhou, H. Liu, Int. J. Hydrogen Energy 28 (2003) 1263–1272.
[20] Z. Qi, A. Kaufman, J. Power Sources 109 (2002) 469–476.
[21] M.V. Williams, H.R. Kunz, J.M. Fenton, J. Power Sources 135 (2004) 122–134.
[22] N.J. Fletcher, C.Y. Chow, E.G. Pow, B. Wozniczka, H.H. Voss, G. Hornburg, D.P. Wilkinson, Canadian Patent No. 2,192,170 (1995).
[23] A. Kumar, R.G. Reddy, J. Power Sources 113 (2003) 11–18.
[24] H. Dohle, R. Jung, N. Kimiaie, J. Mergel, M. Müller, J. Power Sources 124 (2003) 371–384.
[25] F.M. White, Fluid Mechanics, second ed., McGraw Hill, New York, 1986.
[26] H. Wu, X. Li, P. Berg, Int. J. Hydrogen Energy, in press.
[27] S. Maharudrayya, S. Jayanti, A.P. Deshpande, J. Power Sources 138 (2004) 1–13.
[28] R.J. Bellows, M.Y. Lin, M. Arif, A.K. Thompson, D. Jacobson, J. Electrochem. Soc. 146 (1999) 1099–1103.
[29] J. Park, X. Li, D. Tran, T. Abdel-Baset, D.S. Hussey, D.L. Jacobson, M. Arif., Int. J. Hydrogen Energy, submitted for publication.
[30] H. Schlichting, Boundary Layer Theory, seventh ed., McGraw-Hill, 1979.
[31] H. Hassanzadeh, X. Li, J.J. Baschuk, S.H. Mansouri, Int. J. Energy Res., submitted for publication.